PCCP

RSC Publishing

PAPER

View Article Online
View Journal | View Issue

Cite this: *Phys. Chem. Chem. Phys.*, 2013, **15**, 4975

Reactions of the tetraoxidosulfate($^{\bullet-}$) and hydroxyl radicals with poly(sodium α-methylstyrene sulfonate)

Sindy M. Dockheer,†[ab] Lorenz Gubler[b] and Willem H. Koppenol*[a]

Received 3rd December 2012,
Accepted 4th February 2013

DOI: 10.1039/c3cp44341h

www.rsc.org/pccp

Poly(α-methylstyrene sulfonic acid) (PAMS) represents a class of polymers that can form the protogenic constituent in electrolyte membranes for fuel cells. Oxidative stress is thought to play an important role in the degradation of the fuel cell membranes. Having previously established that damage may be mediated *via* abstraction of a benzylic hydrogen, we examined model compounds similar to those used before, but with a methyl group at the α-position. We studied the reaction of $HO^{\bullet}$ and $SO_4^{\bullet-}$, generated by pulse radiolysis, with model compounds in aqueous solution, and measured $k = (2 \pm 0.5) \times 10^{10}$ M^{-1} s^{-1} and $(2 - 3) \times 10^{10}$ M^{-1} s^{-1} for the reaction of $HO^{\bullet}$ with PAMS with average molecular weights of 2640 Da (PAMS-2640) and 6440 Da (PAMS-6440), respectively, at room temperature. At low pH, the decay of the hydroxycyclohexadienyl radical thus formed is accompanied by the formation of an absorption band in the visible region of the spectrum, which we tentatively assign to the radical cation of PAMS-2640 and -6440. The radical cation of PAMS-2640, formed by the reaction of $SO_4^{\bullet-}$ with $k = (6 \pm 1) \times 10^8$ M^{-1} s^{-1}, has a local absorption maximum at 560 nm, with $\varepsilon_{560} \geq 1400$ M^{-1} cm^{-1}. For the reaction of $HO^{\bullet}$ and $SO_4^{\bullet-}$ with the model compound benzenesulfonate, we measured $k = (4–5) \times 10^9$ M^{-1} s^{-1} and $(1.0 \pm 0.3) \times 10^8$ M^{-1} s^{-1}, respectively, while the reaction of $SO_4^{\bullet-}$ with PAMS-6440 proceeds with $(0.8–1) \times 10^9$ M^{-1} s^{-1}. The 4-sulfophenoxyl radical was generated *via* the reaction of $N_3^{\bullet}$ with 4-hydroxybenzenesulfonate; $\varepsilon_{410} \geq 2300$ M^{-1} cm^{-1}. Not unexpectedly, the radical cation of PAMS is longer-lived than that of polystyrene sulfonic acid. Furthermore, fragmentation may result in desulfonation.

Introduction

Fuel cell membranes that contain poly(styrene sulfonic acid)‡ as the protogenic constituent are relatively short-lived under the harsh conditions of an operating fuel cell if the graft component is not adequately crosslinked.[1] Attack of radicals ($HO^{\bullet}$, $H^{\bullet}$ and $HOO^{\bullet}$) on the membrane is considered to initiate membrane decomposition.[2–9] Of these, the most reactive is the $HO^{\bullet}$ radical. Its reaction with aromatic compounds leads to a HO-adduct§ (reaction (1), shown for PAMS) with a yield of *ca.* 90%, followed, at low pH, and in the absence of molecular oxygen, by an acid-catalyzed water elimination to generate a radical cation (reaction (2)).[10–13] In the presence of dissolved O_2, the HO-adduct can be temporarily stabilized by reaction with O_2 to yield a peroxyl radical, which then may decay to phenol and $HOO^{\bullet}$.[12] It was estimated that with such oxygen concentrations as present in the polymer electrolyte of fuel cells, the yield of the phenolic product could be significant.[14] Nevertheless, the formation of benzyl radicals is of importance, in particular in areas of the membrane with low oxygen concentration, *i.e.*, close to the anode. Therefore, the studies of radical attack on styrenic oligomers reported here were carried out in the absence of oxygen.

To study the formation and decay of radical cations, we use $SO_4^{\bullet-}$,[15] which yields the radical cation rapidly and directly (reaction (3), Scheme 1).[16]

Depending on the substituents, radical cations are prone to fragmentation,[17–21] loss of a proton,[12,13,18,19,22–27] reaction with water to yield hydroxycyclohexadienyl radicals[21,23,27,28] and/or decarboxylation.[29] Reaction of $SO_4^{\bullet-}$ with poly(styrene sulfonate) (PSS) yields benzyl radicals (reaction (4)),[22] which is an important

[a] *Institute of Inorganic Chemistry, Department of Chemistry and Applied Biosciences, Swiss Federal Institute of Technology, Wolfgang-Pauli-Strasse 10, 8093 Zurich, Switzerland. E-mail: koppenol@inorg.chem.ethz.ch; Fax: +41-44-632-1090; Tel: +41-44-632-2875*

[b] *Paul Scherrer Institut, Electrochemistry Laboratory, 5232 Villigen PSI, Switzerland*

† Present address: Alstom, Brown Boveri Str. 7, 5400 Baden.

‡ Systematic name of the monomer and *abbreviation* in italics: 4-ethenylbenzene-1-sulfonic acid, *styrene sulfonic acid*; 4-(1-methylethenyl)benzene-1-sulfonic acid, *α-methylstyrene sulfonic acid*.

§ Systematic name and *abbreviation* in italics: 1-hydroxycyclohexa-2,4-diene-6-yl, *HO-adduct*.

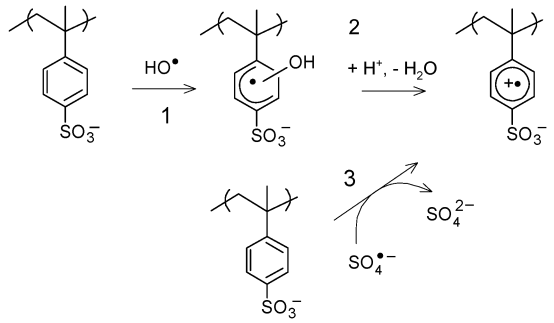

Scheme 1

intermediate in the breakdown of the polymer.

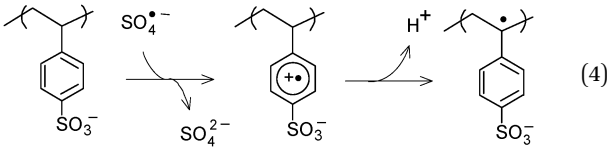

(4)

Hence, this mechanism demonstrates the shortcoming of this compound as a component in fuel cell membranes, because the presence of a weak benzylic C_α-hydrogen, with a bond dissociation energy (BDE) of $\sim$350 kJ mol^{-1},[30] leads to facile H-atom abstraction. However, we could not exclude that heterolytic cleavage of the β-C–C bond of the radical cation also gives rise to benzyl radicals.[21,24,31,32] Such β-fragmentation would constitute a drawback of membranes based on poly(α-methylstyrene sulfonate), which is expected to stabilize the polymer membrane because of the absence of the weak benzylic C_α-hydrogen.[33]

In the present study, we investigate reactions of poly(α-methylstyrene sulfonate) with average molecular weights of 2640 Da (PAMS-2640) and 6440 Da (PAMS-6440) with HO$^\bullet$ and $SO_4^{\bullet-}$. We use pulse radiolysis of aqueous solutions combined with optical detection for the generation and detection of transient species, and HPLC of irradiated solutions of benzenesulfonate to detect the final products. The results allow us to identify differences in the HO$^\bullet$-induced degradation mechanisms of PSS and PAMS.

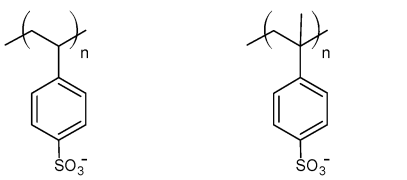

Poly(styrene sulfonate) PSS — Poly(α-methylstyrene sulfonate) PAMS

Materials and methods

Chemicals

PSS-1900, PSS-6800, PAMS-2640 and PAMS-6440 were supplied by PSS (Polymer Standards Service, Mainz, Germany). $HClO_4$ and *tert*-butanol were obtained from Riedel-de-Haën AG (Seelze, Germany) and Merck (Darmstadt, Germany), respectively, while benzenesulfonate (≥99%), $K_2S_2O_8$ (≥99.5%) and acetonitrile (96%, HPLC grade) were supplied by Fluka AG (Buchs SG, Switzerland). Triethylamine (>99.5%) was from Fisher-Scientific AG (Wohlen, Switzerland) and acetic acid (96%, HPLC grade) was purchased from AppliChem (Darmstadt, Germany). NaN_3 (99.99%) and sodium 4-hydroxybenzenesulfonate (>98%) were obtained from Aldrich (Seelze, Germany) and TCI (Eschborn, Germany), respectively. Biphenyl (99.5%) and 4,4′-dihydroxybiphenyl (99%) were supplied by Sigma-Aldrich (Steinheim, Germany).

Pulse radiolysis

The pulse radiolysis experiments were carried out using a Febetron 705 (Titan Systems Corp., presently L-3 Communications, San Leandro, CA, USA), equipped with an optical detection system.[34] Irradiations were performed in a 1 cm quartz cell (Hellma, Mülhausen, Germany) with <50 ns pulses of 2 MeV electrons. The dose was measured using the thiocyanate dosimeter.[35]

Water from a Millipore-Q system was used to prepare solutions that were saturated with air, N_2O, or Ar. The solutions were transferred from a gas-tight syringe (10 ml, Hamilton, SampleLock, Bonaduz, Switzerland) to the measurement cell *via* a syringe pump. pH values of 2.4 and 11 were achieved with $HClO_4$ and NaOH, respectively, while solutions at pH 7 were buffered with 0.1 mM phosphate buffer. Experiments were carried out at room temperature.

Pulse irradiation of water results in the formation of primary species with yields G(HO$^\bullet$), $G(e_{aq}^-)$ and G(H$^\bullet$) of 2.7, 2.65 and 0.6,[35–37] respectively, whereby G = 1 equals 0.1036 μmol generated species per 1 J absorbed energy.

In N_2O-saturated solutions (22 mM (ref. 35–37)), e_{aq}^- reacts according to eqn (5) to yield additional HO$^\bullet$ with $k_5 = 9.1 \times 10^9$ M^{-1} s^{-1}.[36]

$$N_2O + e_{aq}^- + H_2O \rightarrow N_2 + HO^\bullet + HO^- \quad (5)$$

According to eqn (6), the radiation chemical yield G^{N_2O}(HO$^\bullet$-product) in N_2O-saturated solutions depends on [S] and k_S, which denote the substrate concentration and the respective rate constant for the reaction of HO$^\bullet$ with that substrate, respectively, and where the track recombination frequency $\lambda = 4.7 \times 10^8$ s^{-1}.[37]

$$G^{N_2O}(HO^\bullet\text{-product}) = 5.2 + 3.0\frac{(k_S[S]/\lambda)^{0.5}}{1 + (k_S[S]/\lambda)^{0.5}} \quad (6)$$

At pH 2.4, hydrated electrons react with protons to yield additional hydrogen radicals (eqn (7)), $k_7 = 2.3 \times 10^{10}$ M^{-1} s^{-1} (ref. 38) at the expense of reaction (5).

$$e_{aq}^- + H^+ \rightarrow H^\bullet \quad (7)$$

We followed reactions of $N_3^\bullet$ produced *via* reaction (8), $k_8 = 1.2 \times 10^{10}$ M^{-1} s^{-1},[39] with sodium 4-hydroxybenzenesulfonate in N_2O-saturated 0.01 M NaN_3 solutions at pH 11. Thus, eqn (6) predicts $G^{N_2O}(N_3^\bullet) = 6.2$.

$$HO^\bullet + N_3^- \rightarrow HO^- + N_3^\bullet \quad (8)$$

In argon-saturated solutions that contain 0.05 M $S_2O_8^{2-}$, hydrated electrons are converted to $SO_4^{\bullet-}$, $k_9 = 1.2 \times 10^{10}$ M^{-1} s^{-1} (ref. 39) (eqn (9)). The principal reactions in such a solution in the absence of a substrate, with *t*-butanol (*t*-BuOH) as a HO$^\bullet$-scavenger, consist of eqn (7) and (9)–(13), with $k_{10} = 1.4 \times 10^7$ M^{-1} s^{-1},[40] $k_{11} = 6 \times 10^8$ M^{-1} s^{-1},[39] $k_{12} = 8.4 \times 10^5$ M^{-1} s^{-1} (ref. 41) and $k_{13} = 6.1 \times 10^5$ M^{-1} s^{-1}.[42] The yield of the products of scavenging e_{aq}^- *via* eqn (7) and (9) depends on the scavenger concentration and the respective rate constants.[43] Experimentally, we determined a yield $G(SO_4^{\bullet-})$ of (4.0 ± 0.2) in irradiated argon-saturated 0.05 M $K_2S_2O_8$ solutions at pH 2.4 with doses of 10 to 70 Gy.

$$e_{aq}^- + S_2O_8^{2-} \rightarrow SO_4^{\bullet-} + SO_4^{2-} \quad (9)$$

$$H^\bullet + S_2O_8^{2-} \rightarrow SO_4^{\bullet-} + SO_4^{2-} + H^+ \quad (10)$$

$$HO^\bullet + C(CH_3)_3OH \rightarrow H_2O + {}^\bullet CH_2C(CH_3)_2OH \quad (11)$$

$$SO_4^{\bullet-} + C(CH_3)_3OH \rightarrow SO_4^{2-} + {}^\bullet CH_2C(CH_3)_2OH + H^+ \quad (12)$$

$$SO_4^{\bullet-} + S_2O_8^{2-} \rightarrow S_2O_8^{\bullet-} + SO_4^{2-} \quad (13)$$

HPLC

Product analysis was performed with a Hewlett Packard (HP, presently Agilent, Santa Clara, US) 1050 series high performance liquid chromatograph, equipped with an HP 1050 series quarternary pump, an Agilent 1100 series vacuum degasser and an HP 1050 series diode array detector. Separation was performed at ambient temperature (25 °C) on a Macherey-Nagel Nucleodur Sphinx RP column (250 × 4.6 mm, 5 μm particles) under isocratic elution with a mobile phase water–acetonitrile (40 : 60) that contained 5 mM of an ion-pairing agent (acetic acid/triethylamine). After 50 μl injections, 4,4′-dihydroxybiphenyl and biphenyl from standard solutions eluted at 2.9 and 6.5 minutes, respectively, at a flow rate of 1 ml min^{-1}.

Results

Reactions in N_2O-saturated solution

To study the reaction of HO$^\bullet$ with PAMS-2640 (reaction (1)) we irradiated a deoxygenated N_2O-saturated solution of 1 mM PAMS-2640 at pH 7. The absorption spectrum of mainly HO-adducts (10% H-adducts, eqn (14)) of PAMS-2640, obtained 1 μs after the pulse, has a maximum near 340 nm, Fig. 1. We followed the rate of formation of the HO-adducts at 320–350 nm during the first 2–6 μs at various [PAMS-2640]. With least-squares analysis we can accurately fit the increase of absorbance to an exponential function; from a plot of pseudo-first-order rate constants as a function of [PAMS-2640] (Fig. 2), we derive $k_1 = (2.0 \pm 0.5) \times 10^{10}$ M^{-1} s^{-1} (Table 1).

Based on k_1 and a concentration of 1 mM PAMS-2640, eqn (6) predicts that G^{N_2O}(HO-adduct) = 5.7 and we derive G(adducts) = G^{N_2O}(HO-adduct) + G(H-adducts) = 5.7 + 0.6 = 6.3. With the observed maximal absorbance of 2.8×10^{-3} absorbance units (AU) per Gy at 340 nm, we calculated an average $\varepsilon_{340} = (4.3 \pm 0.4) \times 10^{-3}$ M^{-1} cm^{-1}, in agreement with an earlier determination.[44] The error is based on a 10% uncertainty in the dose.

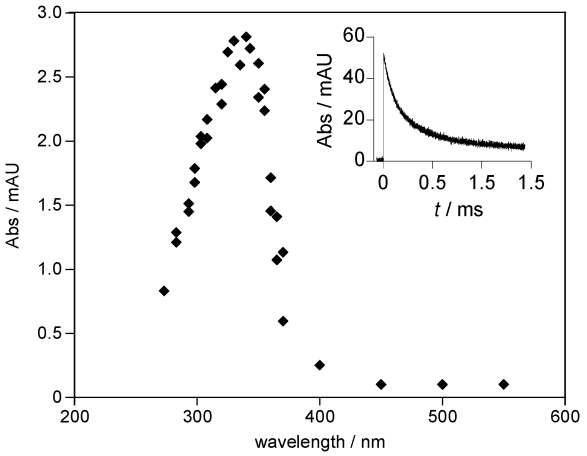

Fig. 1 Transient absorption spectrum of HO- and H-adducts of PAMS-2640, normalized to 1 Gy and constructed from time resolved absorbance values 1 μs after the pulse. Obtained from irradiated (dose 15–20 Gy) N_2O-saturated solutions that contain 1 mM PAMS-2640 at pH 7, with 0.1 mM phosphate buffer. Inset: change of optical density at 340 nm shows formation and decay of adducts at a dose of 18 Gy.

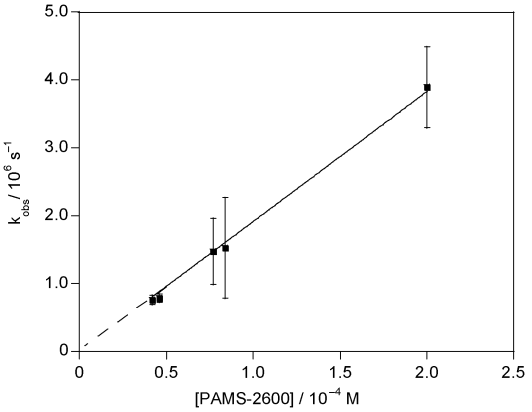

Fig. 2 Pseudo-first-order rate constants, evaluated at 320–350 for the reaction of HO$^\bullet$ with PAMS-2640 as a function of concentration at room temperature; solutions purged with N_2O, irradiated (dose 10–15 Gy) at pH 7, with 0.1 mM phosphate buffer.

The decay of absorbance assigned to the adducts of PAMS-2640 (Fig. 1, inset) follows second-order kinetics with $2k/\varepsilon_{340} = (1.3 \pm 0.2) \times 10^5$ cm s^{-1}, from which we derived a second-order rate constant of $(2.8 \pm 0.7) \times 10^8$ M^{-1} s^{-1}.

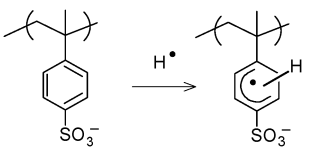

(14)

We carried out similar experiments to study the reaction of HO$^\bullet$ with benzenesulfonate and PAMS-6440 by following the increase in absorbance at 320–340 nm from N_2O-saturated solutions that contained 0.2–0.5 mM benzenesulfonate or

Table 1 Rate constants for reaction of $HO^{\bullet}$ and $SO_4^{\bullet -}$ with PAMS-2640, PAMS-6440, PSS-1100 and benzenesulfonate

	$HO^{\bullet}$		$SO_4^{\bullet -}$	
Substrate	Substrate concentration [mM]	k [M^{-1} s^{-1}]	Substrate concentration [mM]	k [M^{-1} s^{-1}]
PAMS-2640	0.04–0.2	$(2.0 \pm 0.5) \times 10^{10}$	0.5–2	$(6 \pm 1) \times 10^{8}$ [a]
PAMS-6400	0.01, 0.02	$(2–3) \times 10^{10}$	0.1, 0.2	$(0.8–1) \times 10^{9}$
PSS-1100[a]	0.03–0.3	$(9.5 \pm 0.6) \times 10^{9}$	0.5–2.5	$(4.5 \pm 0.6) \times 10^{8}$
Benzenesulfonate	0.2–0.5	$(4–6) \times 10^{9}$	2–5	$(1.0 \pm 0.3) \times 10^{8}$

[a] Ref. 22.

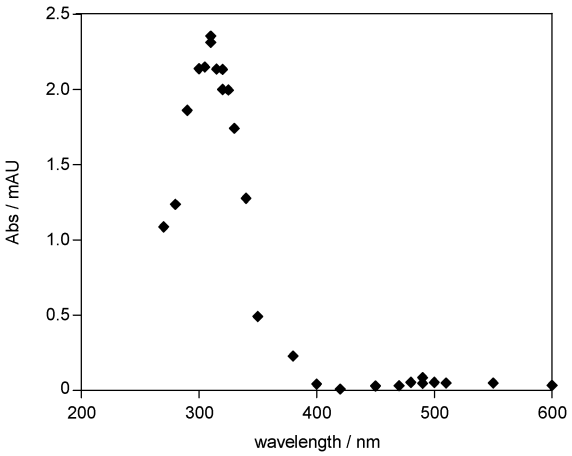

Fig. 3 Absorption spectrum of HO- and H-adducts of benzenesulfonate, 5 μs after the pulse (15–20 Gy), in N_2O-saturated 0.2 mM benzenesulfonate solutions at pH 7, with 0.1 mM phosphate buffer.

0.01 and 0.02 mM PAMS-6440 at pH 7; the rate constants we obtained are $k = (4–6) \times 10^{9}$ M^{-1} s^{-1} and $(2–3) \times 10^{10}$ M^{-1} s^{-1}, respectively (Table 1). A normalized spectrum of the adducts of benzenesulfonate is shown in Fig. 3.

At pH 2.4, the spectra obtained 4, 30 and 130 μs after pulse irradiation of a 0.08 mM PAMS-2640 N_2O-saturated solution (Fig. 4) indicate the initial formation of HO- and H-adducts of PAMS-2640, which subsequently decay. As shown in Fig. 5

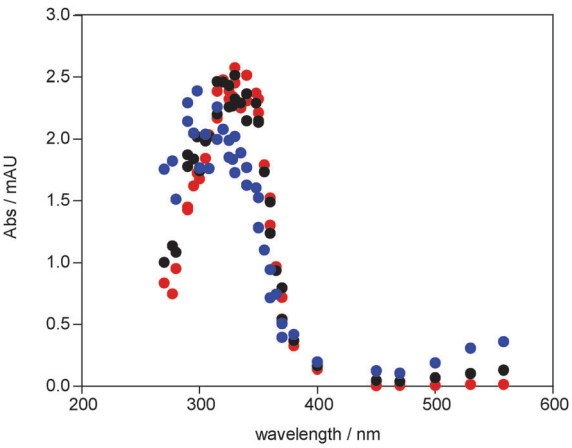

Fig. 4 Transient absorption spectra illustrating the formation and decay of HO- and H-adducts of PAMS-2640 at pH 2.4, constructed from time-resolved absorbance readings, normalized to 1 Gy, 4 (●), 30 (●) and 130 (●) μs after irradiation (8–12 Gy) of 0.08 mM PAMS-2640 solutions, purged with N_2O.

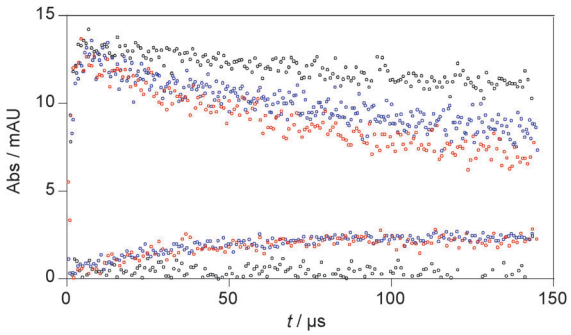

Fig. 5 Changes in optical density at 340 nm (upper traces) and 550 nm (lower traces) represent the formation and decay of HO- and H-adducts. Black, PAMS-2460, 0.08 mM, pH 7; red: PAMS-2640, 0.08 mM, pH 2.4; blue, PAMS-6400, 0.02 mM, pH 2.4. Irradiation dose 5–10 Gy, solutions purged with N_2O, pH 7.

(upper curves), the decay of adducts of PAMS-2640 is faster at pH 2.4 than at pH 7 and somewhat faster than the decay of adducts of PAMS-6440 at pH 2.4. In addition, as seen in Fig. 4 and 5, a change in pH from 7 to 2.4 brought about the appearance of an absorbance in the visible region of the spectrum in the case of PAMS-2640. In analogy, the decay of the absorbance of adducts of PAMS-6440 at 340 nm is accompanied by the appearance of an absorbance in the visible region of the spectrum on the same time scale (Fig. 5). This absorbance did not develop at pH 2.4 when 0.2 M *t*-BuOH was added as a $HO^{\bullet}$-scavenger.

Reactions with $SO_4^{\bullet -}$

We generated $SO_4^{\bullet -}$ in Ar-saturated solutions that contained 0.05 M $K_2S_2O_8$ at pH 2.4 and followed its reaction with 1 mM PAMS-2640. The transient spectra we observed 1 and 10 μs after the pulse are shown in Fig. 6. 0.1 M *t*-BuOH was included to scavenge most of the $HO^{\bullet}$ radicals *via* reaction (11). Experiments with and without *t*-BuOH confirmed the scavenging of $HO^{\bullet}$ by *t*-BuOH, because we observed a significant decrease in the absorbance at 320 to 340 nm if 0.1 M *t*-BuOH was present. As shown in Fig. 6, an absorption with local maxima at 340 and 560 nm appears, and between 1 to 10 μs, the maximum at 340 nm shifts to 300 nm.

Fig. 7 demonstrates that formation of the absorption at 560 nm does not depend on $[O_2]$. Therefore, in the experiments that resulted in Fig. 8 and 9, we used aerated solutions to follow the reaction of $SO_4^{\bullet -}$ with PAMS-2640, PAMS-6440, PSS-1920, PSS-6800 and benzenesulfonate at wavelengths in the visible region of the spectrum. Fig. 8 and 9 show traces at 560 and 650 nm. When 0.5 mM PAMS-2640 or 0.2 mM PAMS-6440 was present, we observe the development of absorptions at 550 to 650 nm

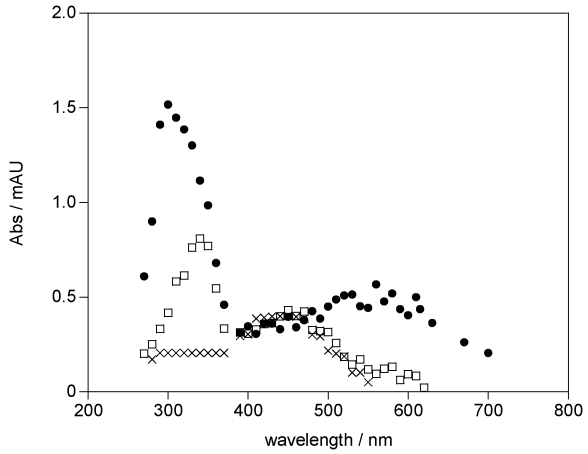

Fig. 6 Transient absorption spectra 1 (□) and 10 (●) μs after the pulse (dose 10–15 Gy), obtained from time-resolved absorbance readings, normalized to 1 Gy, measured in argon-saturated solutions that contained 1 mM PAMS-2640, 0.05 M $K_2S_2O_8$ and 0.1 M *t*-BuOH at pH 2.4. A scaled spectrum of $SO_4^{\bullet-}$ (×) from ref. 45 and based on $G = 4$ shows the contribution of $SO_4^{\bullet-}$ 1 μs after the pulse.

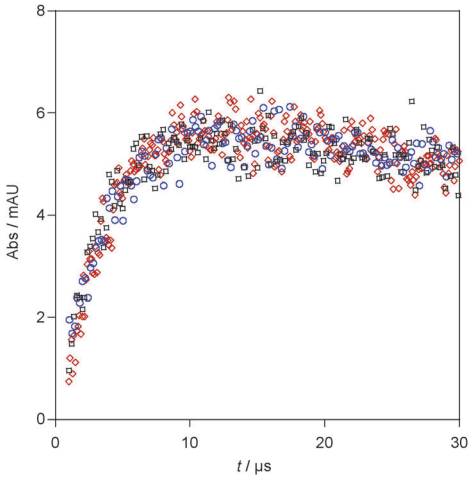

Fig. 7 Change in optical density at 560 nm in a (□) deoxygenated, argon-saturated solution and in the presence of 0.26 (○) and 0.60 (◊) mM O_2. Traces were normalized to 12 Gy and were obtained from pulse irradiated 0.05 M $K_2S_2O_8$, 0.5 mM PAMS-2640 solutions at pH 2.4.

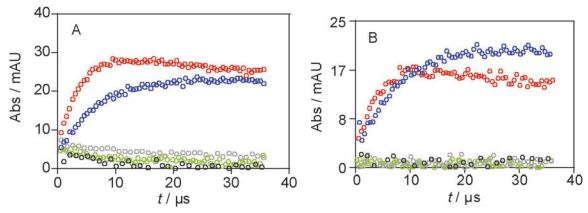

Fig. 8 Change of optical density at (A) 560 nm and (B) 650 nm within the first 40 μs after the pulse, observed in irradiated (dose of *ca.* 50–55 Gy) aerated 0.05 M $K_2S_2O_8$ solutions that contained: red, 0.5 mM PAMS-2640; blue, 0.2 mM PAMS-6440; green, 0.4 mM PSS-1920; grey, 0.1 mM PSS-6800, and black, 2.5 mM benzenesulfonate at pH 2.4.

within the first 10 μs after the pulse from irradiated aerated 0.05 M $K_2S_2O_8$ solutions at pH 2.4. Fig. 8 and 9 illustrate the same

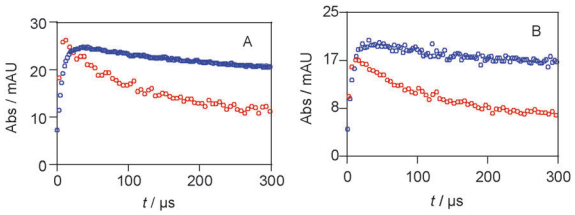

Fig. 9 Course of absorbance followed at (A) 560 nm and (B) 650 nm within the first 300 μs after the pulse, observed in aerated 0.05 M $K_2S_2O_8$ solutions that contained (red) 0.5 mM PAMS-2640 and (blue) 0.2 mM PAMS-6440 at pH 2.4, irradiated with a dose of 50–55 Gy.

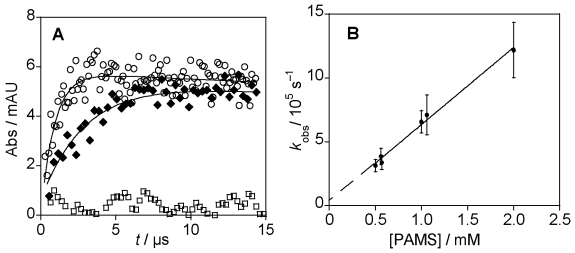

Fig. 10 (A) Development and decrease of absorbance followed at 560 nm, in the absence (□) of PAMS-2640 and in the presence of 0.5 (◆) and 2 (○) mM PAMS-2640, in argon-saturated 0.05 M $K_2S_2O_8$ solutions, irradiated with doses of 8–12 Gy at pH 2.4. (B) Pseudo-first-order rate constants, evaluated at 550–570 nm, obtained from irradiated argon-saturated 0.05 M $K_2S_2O_8$ solutions as a function of concentration, at room temperature, $I = 0.2$–0.29 M.

time dependence of the absorbance at 560 and 650 nm when 0.5 mM PAMS-2640 or 0.2 mM PAMS-6440 was present. Conversely, in analogous experiments with 2.5 mM benzenesulfonate, 0.4 mM PSS-1920 or 0.1 mM PSS-6800, we note the development of significantly lower absorbances between 560 nm and 650 nm (Fig. 8).

For PAMS-2640 and PAMS-6440, the rate of formation of the absorbance at 560–650 nm depends on the concentration, which is illustrated in Fig. 10A for PAMS-2640. Fig. 10B displays the linear correlation of the pseudo-first order rate constants, evaluated at 550–650 nm, as a function of [PAMS-2640], from which we derived a second-order rate constant of $(6 \pm 1) \times 10^8$ M^{-1} s^{-1}. In similar experiments with PAMS-6440, we calculated a second-order rate constant of $(0.8\text{–}1) \times 10^9$ M^{-1} s^{-1}.

The rate of decay of the absorption of transients of PAMS-2640 in the visible region of the spectrum depends on the dose (20–50 Gy), which indicates a second-order component in the decay, while the transients of PAMS-6440 decay significantly slower, as illustrated in Fig. 9 at doses of 50–55 Gy.

We investigated whether the phenyl radical is formed (reaction (15)) during the reaction of $SO_4^{\bullet-}$ with benzenesulfonate. This model compound lacks an alkyl substituent and we investigated by HPLC whether dihydroxybiphenyl is formed in aerated solutions according to eqn (16).[46]

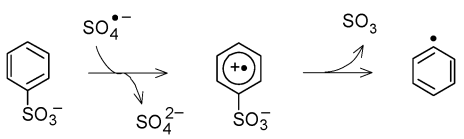

(15)

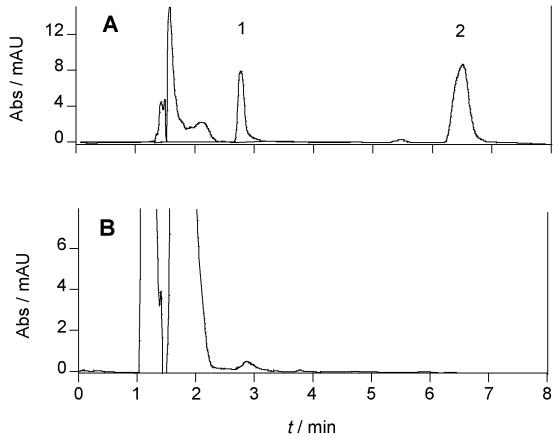

Fig. 11 HPLC chromatogram of (A) standard solutions that contained (1) 1.5 μM dihydroxybiphenyl and (2) 3.5 μM biphenyl and (B) a pulse irradiated aerated solution that contained 2.5 mM benzenesulfonate, 0.02 M $K_2S_2O_8$ and 0.05 M *t*-BuOH at pH 4. The injection volume was 50 μl, a flow rate of 1 ml min^{-1}, isocratic elution with 60 : 40 acetonitrile : water.

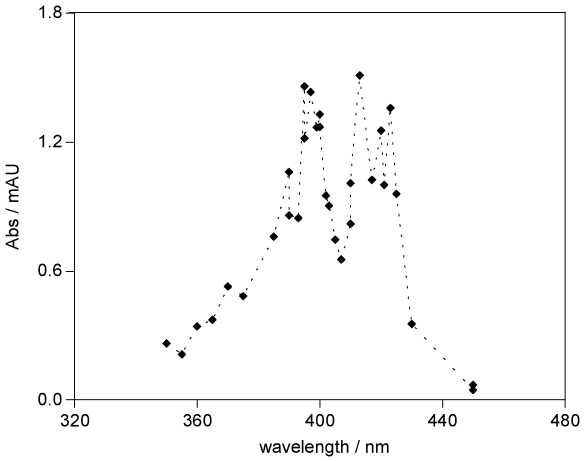

Fig. 12 Transient absorption spectrum, normalized to 1 Gy, of the *p*-sulfophenoxyl radical upon oxidation of 0.6 mM sodium 4-hydroxybenzenesulfonate by $N_3^\bullet$ at pH 11 in a N_2O-saturated 0.01 M NaN_3 solution (irradiation dose 10–15 Gy), 4 μs after the pulse.

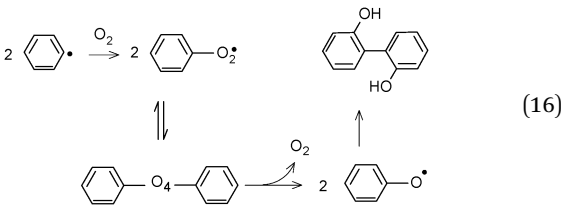

(16)

We analysed the products of pulse-irradiated aerated solutions (160–170 Gy) that contained 2.5 mM benzenesulfonate, 0.02 M $S_2O_8^{2-}$ and 0.05 M *t*-BuOH at pH 4 by HPLC. 500 μl of irradiated samples were transferred to sample vials; these contained 1.5 ml methanol to dilute dihydroxybiphenyl and biphenyl, which are not very soluble, and were immediately sealed to prevent evaporation of products. Fig. 11 shows the chromatograms of solutions that contained 1.5 μM dihydroxybiphenyl and 3.5 μM biphenyl and of the irradiated solution obtained under isocratic elution. The HPLC chromatogram shows the presence of a small peak at 2.9 minutes, which we assign to dihydroxybiphenyl (Fig. 11B).

Based on a *G* value of 4 for $SO_4^{\bullet-}$, a dose of 160–170 Gy, and 100% conversion to phenyl radical and to dihydroxybiphenyl, 20 μM of the latter is expected. With *ca.* 0.15 μM found, the yield is of the order of 1%.

Reaction of $N_3^\bullet$ with 4-hydroxybenzenesulfonate

We used the oxidation of 4-hydroxybenzenesulfonate by $N_3^\bullet$ according to eqn (17) to produce the phenoxyl radical.[47] Fig. 12 displays the transient absorption spectrum of the *p*-sulfophenoxyl radical, which we observed 4 μs after pulse irradiation (10–15 Gy) of a 0.01 M NaN_3, N_2O-saturated solution that contained 0.6 mM 4-hydroxybenzesulfonate at pH 11. Based on G^{N_2O}(HO$^\bullet$-product) = $G^{N_2O}(N_3^\bullet)$ 6.2 and a local maximum of 1.5×10^{-3} AU (Fig. 12), we obtained an estimate for the extinction coefficient of $\varepsilon_{410} = (2.3 \pm 0.2)\ M^{-1}\ cm^{-1}$. Depending on the rate of reaction (17), this value represents a lower limit because of the fast recombination of $N_3^\bullet$ radicals according to eqn (18), with $k_{18} = 4.4 \times 10^9\ M^{-1}\ s^{-1}$,[47] and because of the second-order decay of the phenoxyl radicals.[48] The magnitude of ε_{max} is slightly lower than that found in the literature,[49] but the spectrum with distinct peaks at 395 nm and at around 415 nm agrees with that of other phenoxyl radicals.[47,49]

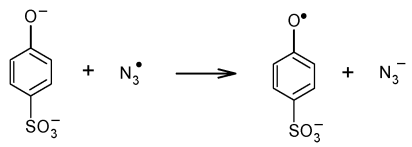

(17)

$$N_3^\bullet + N_3^\bullet \rightarrow 3N_2 \qquad (18)$$

Discussion

The nearly diffusion-limited reaction of HO$^\bullet$ with PAMS-2640 and PAMS-6440 generates HO-adducts according to reaction (1). At pH 2.4, the decay of HO-adducts is accompanied by the development of an absorbance in the visible region of the spectrum, which does not arise if HO$^\bullet$ is scavenged by *t*-BuOH, or if the reaction is carried out in neutral solutions. These observations point to reaction (2), the acid-catalyzed transformation of the HO-adduct to a radical cation.[11–13] It thus became necessary to study these radical cations directly. Based on spectral and kinetics data in combination with literature values, we suggest that the initial product of the oxidation of PAMS-2640 and PAMS-6440 by $SO_4^{\bullet-}$ is indeed the aromatic radical cation of the parent compounds (reaction (3)), whose formation and decay could be observed because of its appreciable absorbance in the visible region of the spectrum, as discussed below.

Regarding the reaction of $SO_4^{\bullet-}$ with PAMS-2640, we assign the initial absorbance 1 μs after the pulse in Fig. 6 to both formation of $SO_4^{\bullet-}$ and H- and HO-adducts of the parent compound. Formation of adducts cannot be completely prevented because of incomplete scavenging of HO$^\bullet$ and H$^\bullet$.

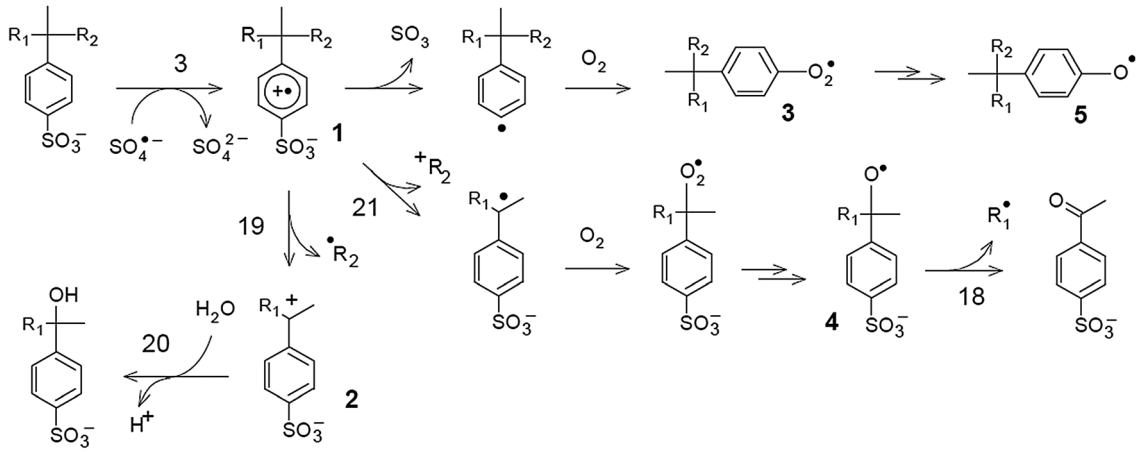

Scheme 2

A scaled spectrum of $SO_4^{\bullet -}$,[45] based on $G(SO_4^{\bullet -}) = 4$, is included in Fig. 6 and indicates a contribution of 0.2×10^{-3} AU per Gy at 340 nm by adducts. From the difference $\Delta Abs_{340\ nm}$ of 0.6 and given ε_{340}(adducts) = $4.3 \times 10^3\ M^{-1}\ cm^{-1}$, we derive G(adducts) = 1.4.

The spectrum 10 μs after the pulse is characterized by a maximum at around 300 nm and a broad absorption in the visible region of the spectrum, whose maximum is centered at around 560 nm (Fig. 6). Transient species that exhibit broad absorptions in this wavelength region include radical cations (**1**, Scheme 2),[11,12,50–52] benzyl cations (**2**, Scheme 2),[53–55] phenylperoxyl radicals (**3**, Scheme 2),[56–61] and cumyloxyl type radicals (**4**, Scheme 2).[62] Feasible pathways of formation of these transients upon reaction of $SO_4^{\bullet -}$ with PAMS-2640 are shown in Scheme 2. Given the independence of formation of the transient on [O_2] (Fig. 7), we exclude radicals **3**, **4** and **5**. Moreover, cumyloxyl radicals (analogous to **4**) are short-lived due to a fast β-fragmentation that proceeds with $k = 10^7\ s^{-1}$ in aqueous solution.[63] (Scheme 2, reaction (18)). Further, the absence of a characteristic signature at around 400 nm in Fig. 6 (according to Fig. 12) confirms the absence of a phenoxyl type radical, **5**.

Both aromatic radical cations **1** and benzyl cations **2** exhibit absorptions in the visible region of the spectrum. The latter may be formed *via* a fast heterolytic cleavage of the β-C–C bond of the radical cation according to reaction (19), Scheme 2. However, we may expect the benzyl cation to be too short-lived to be observed in aqueous solution due to reaction (20), Scheme 2, which, in the case of Ph_2CH^+, is reported to proceed with a k of $1.2 \times 10^8\ M^{-1}\ s^{-1}$.[64] On the other hand, charge resonance may stabilize the benzylic cation. Reactions 19 and 21 would result in bond scission of the polymer.

We suggest that formation of the radical cation *via* reaction (3) accounts for the appearance of the absorption in the visible region of the spectrum. Accordingly, we assign the rate constant k of $(6 \pm 1) \times 10^8\ M^{-1}\ s^{-1}$ (Table 1) to the reaction of $SO_4^{\bullet -}$ with PAMS-2640 (reaction (3)). This assignment would also hold if benzyl cations instead of aromatic radical cations account for the absorption in the visible region, because, in that case, reaction (3) would be rate-limiting. Rate constants for the reactions of $HO^{\bullet}$ and $SO_4^{\bullet -}$ with PAMS-2640 and benzenesulfonate, respectively, are compiled for comparison with PSS-1100 in Table 1.

Thus, the radical cation of PAMS-2640 and PAMS-6440 appears to be longer-lived than the radical cation of PSS-1100.[15] We observed that the development and decay of the absorbance in the visible region of the spectrum is independent of [O_2], which agrees with data on the radical cation of 9-hydroxyfluorene.[51]

Charge resonance and formation of dimer radical cations are thought to stabilize radical cations of aromatic systems,[20,50,51,65–67] for instance, in the case of diarylethane.[19] For the radical cations of 9H-fluorene and 9,10-dihydrophenanthrene, extinction coefficients on the order of $10^4\ M^{-1}\ cm^{-1}$ at 640 nm have been reported.[50] The intermolecular addition of radical cations of benzene, toluene and naphthalene to their parent compound was assigned second-order rate constants of $k \leq 3 \times 10^8\ M^{-1}\ s^{-1}$ and $k \leq 10^9\ M^{-1}\ s^{-1}$ (ref. 20) which supports the idea of a mechanism that involves intramolecular addition of a radical cation to another vicinal aromatic ring in the coiled structure of the polymer (Fig. 13).

The decay of the absorption that we believe to be due to the radical cation of PAMS-2640 is of mixed second- and first-order kinetics. The second-order decay of radical cations of methoxybenzenes proceeds with rate constants on the order of $10^9\ M^{-1}\ s^{-1}$.[11] As seen in Fig. 8 and 9, the decay of the transient absorption at 560 and 650 nm is slower with higher MW poly(α-methylstyrene sulfonate), which may be rationalized with the lower mobility of the higher MW polymer and with the higher probability of intramolecular reactions.

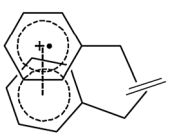

Fig. 13 A radical cation may be stabilised by forming an adduct to another α-methylstyrene sulfonic acid.

In the experiments that lead to Fig. 6, $SO_4^{\bullet -}$ is formed with $G = 4$ and disappears *via* reactions (3), (12) and (13), which results in a yield G(radical cation) $\approx 0.84 \times 4 = 3.4$. With 0.5×10^{-3} AU at 560 nm (Fig. 6), we derive an estimate $\varepsilon_{560} \geq 1400\ M^{-1}\ cm^{-1}$, which we take as a lower limit because of the second-order decay of radical cations, with rate constants on the order of $10^9\ M^{-1}\ s^{-1}$ as found for monomer radical cations.[11]

Apart from the dose-dependent second-order decay, our data do not allow us to conclude *via* which reactions the radical cations further decay at low radical concentration. Thus, the products of subsequent reactions of the radical cations of PAMS-2640 and PAMS-6440 are unknown at present. There is, however, a hint: the HPLC chromatogram shows that a minor product of benzenesulfonate oxidation by $SO_4^{\bullet -}$ is dihydroxybiphenyl (Fig. 11). This finding is consistent with reaction (15), followed by reaction (16), which involves loss of SO_3 and subsequent formation of dihydroxybiphenyl in low yield. In the case of benzoate, the loss of CO_2 from the radical cation with formation of a phenyl radical amounted to 70% of the initial radical cation production.[29] A mechanism that includes loss of SO_3 from a radical cation of the parent compound would be particularly harmful for fuel cell membranes because of the direct loss of the protogenic constituent and, thus, the proton-conductivity of membranes.

References

1 L. Gubler and G. G. Scherer, *Polymer Electrolyte Fuel Cell Durability*, ed. M. Inaba, T. J. Schmidt and F. N. Büchi, Springer Science+Business Media, New York, 2009, pp. 133–155.
2 R. Borup, J. Meyers, B. Pivovar, Y. S. Kim, R. Mukundan, N. Garland, D. Myers, M. Wilson, F. Garzon, D. Wood, P. Zelenay, K. More, K. Stroh, T. Zawodzinski, J. Boncella, J. E. McGrath, M. Inaba, K. Miyatake, M. Hori, K. Ota, Z. Ogumi, S. Miyata, A. Nishikata, Z. Siroma, Y. Uchimoto, K. Yasuda, K. i. Kimijima and N. Iwashita, *Chem. Rev.*, 2007, **107**, 3904–3951.
3 A. Collier, H. Wang, X. Z. Yuan, J. Zhang and D. P. Wilkinson, *Int. J. Hydrogen Energy*, 2006, **31**, 1838–1854.
4 F. D. Coms, *ECS Trans.*, 2008, **16**, 235–255.
5 M. Danilczuk, F. D. Coms and S. Schlick, *J. Phys. Chem. B*, 2009, **113**, 8031–8042.
6 H. Liu, F. D. Coms, J. Zhang, H. A. Gasteiger and A. B. LaConti, *Polymer Electrolyte Fuel Cell Durability*, ed. F. N. Büchi, Springer Science+Business, 2009, pp. 71–118.
7 Y. Nosaka, K. Ohtaka, M. Kitazawa, S. Kishioka and A. Y. Nosaka, *Electrochem. Solid-State Lett.*, 2009, **12**, B14–B17.
8 N. Ohguri, A. Y. Nosaka and Y. Nosaka, *Electrochem. Solid-State Lett.*, 2009, **12**, B94–B96.
9 N. Ohguri, A. Nosaka and Y. Nosaka, *J. Power Sources*, 2010, **195**, 467.
10 D. Behar and J. Rabani, *J. Phys. Chem.*, 1988, **92**, 5288–5292.
11 P. O'Neill, S. Steenken and D. Schulte-Frohlinde, *J. Phys. Chem.*, 1975, **79**, 2773–2779.
12 K. Sehested, J. Holcman and E. J. Hart, *J. Phys. Chem.*, 1977, **81**, 1363–1367.
13 K. Sehested and J. Holcman, *J. Phys. Chem.*, 1978, **82**, 851–853.
14 L. Gubler, S. M. Dockheer and W. H. Koppenol, *J. Electrochem. Soc.*, 2011, **158**, B755–B769.
15 S. M. Dockheer, L. Gubler, A. Wokaun and W. H. Koppenol, *Phys. Chem. Chem. Phys.*, 2011, **13**, 12429–12434.
16 P. Neta, V. Madhavan, H. Zemel and R. W. Fessenden, *J. Am. Chem. Soc.*, 1977, **99**, 163–165.
17 E. Baciocchi, M. Bietti and O. Lanzalunga, *Acc. Chem. Res.*, 2000, **33**, 243–251.
18 E. Baciocchi, M. Bietti and O. Lanzalunga, *J. Phys. Org. Chem.*, 2006, **19**, 467–468.
19 D. M. Camaioni and J. A. Franz, *J. Org. Chem.*, 1984, **49**, 1607–1613.
20 T. N. Das, *J. Phys. Chem. A*, 2009, **113**, 6489–6493.
21 S. Steenken and R. A. McClelland, *J. Am. Chem. Soc.*, 1989, 111.
22 S. Dockheer, L. Gubler, P. L. Bounds, A. S. Domazou, G. G. Scherer, A. Wokaun and W. H. Koppenol, *Phys. Chem. Chem. Phys.*, 2010, **12**, 11609–11616.
23 C. Russo-Caia and S. Steenken, *Phys. Chem. Chem. Phys.*, 2002, **4**, 1478–1485.
24 C. Walling, C. Zhao and G. M. El-Taliawi, *J. Org. Chem.*, 1983, **48**, 4910–4914.
25 M. K. Eberhardt, *J. Org. Chem.*, 1977, **42**, 832–835.
26 F. Minisci, A. Citterio and C. Giordano, *Acc. Chem. Res.*, 1983, **16**, 27–32.
27 C. Walling, D. M. Camaioni and S. S. Kim, *J. Am. Chem. Soc.*, 1978, **100**, 4814–4818.
28 S. Steenken, *J. Chem. Soc., Faraday Trans. 1*, 1987, **83**, 113–124.
29 H. Zemel and R. W. Fessenden, *J. Phys. Chem.*, 1978, **82**, 2670–2676.
30 Y. R. Luo, *Comprehensive Handbook of Chemical Bond Energies*, CRC Press, Boca Raton, Florida, 2007.
31 E. Baciocchi, M. Bietti, L. Manduchi and S. Steenken, *J. Am. Chem. Soc.*, 1999, **121**, 6624–6629.
32 E. Baciocchi, D. Bartoli, C. Rol, R. Ruzziconi and G. V. Sebastiani, *J. Org. Chem.*, 1986, **51**, 3587–3593.
33 L. Gubler, M. Slaski, F. Wallasch, A. Wokaun and G. G. Scherer, *J. Membr. Sci.*, 2009, **339**, 68–77.
34 T. Nauser, G. Casi, W. H. Koppenol and C. Schöneich, *J. Phys. Chem. B*, 2008, **112**, 15034–15044.
35 R. H. Schuler, L. K. Patterson and E. Janata, *J. Phys. Chem.*, 1980, **84**, 2088–2089.
36 C. von Sonntag, *The Chemical Basis of Radiation Biology*, Taylor & Francis, London, 1987.
37 R. H. Schuler, A. L. Hartzell and B. Behar, *J. Phys. Chem.*, 1981, **85**, 192–199.
38 A. J. Elliot, D. R. McCracken, G. V. Buxton and N. D. Wood, *J. Chem. Soc., Faraday Trans.*, 1990, **86**, 1539–1547.
39 G. V. Buxton, C. L. Greenstock, W. P. Helman and A. B. Ross, *J. Phys. Chem. Ref. Data*, 1988, **17**, 513–886.
40 R. W. Matthews, H. A. Mahlmann and T. J. Sworski, *J. Phys. Chem.*, 1970, **74**, 2475–2479.

41 C. L. Clifton and R. E. Huie, *Int. J. Chem. Kinet.*, 1989, **21**, 677–687.
42 W. J. McElroy and S. J. Waygood, *J. Chem. Soc., Faraday Trans.*, 1990, **86**, 2557–2564.
43 T. I. Balkas, J. H. Fendler and R. H. Schuler, *J. Phys. Chem.*, 1970, **74**, 4497–4505.
44 K. Sehested, H. Corfitzen, H. C. Christensen and E. J. Hart, *J. Phys. Chem.*, 1975, **79**, 310–315.
45 E. Hayon, A. Treinin and J. Wilf, *J. Am. Chem. Soc.*, 1972, **94**, 47–57.
46 P. Neta and S. Steenken, *The Chemistry of Phenols*, ed. Z. Rappoport, John Wiley & Sons, Chichester, ch. 152003.
47 Z. B. Alfassi and R. H. Schuler, *J. Phys. Chem.*, 1985, **89**, 3359–3363.
48 A. S. Domazou, W. H. Koppenol and J. M. Gebicki, *Free Radical Biol. Med.*, 2009, **46**, 1049–1057.
49 S. Steenken and P. Neta, *The Chemistry of the Phenols*, ed. Z. Rappoport, John Wiley & Sons, Chichester, 2003, ch. 16.
50 M. O. Delcourt and M. J. Rossi, *J. Phys. Chem.*, 1982, **86**, 3233–3239.
51 R. A. McClelland, N. Mathivanan and S. Steenken, *J. Am. Chem. Soc.*, 1990, **112**, 4857–4861.
52 H. Mohan and J. P. Mittal, *Chem. Phys. Lett.*, 1996, **263**, 263–270.
53 N. Fujisaki, P. Comte and T. Gäumann, *Ber. Bunsen-Ges. Phys. Chem. Chem. Phys.*, 1994, **98**, 1256–1262.
54 J. A. Grace and M. C. R. Symons, *J. Chem. Soc.*, 1959, 958–962.
55 R. A. McClelland, V. M. Kanagasabapathy and S. Steenken, *J. Am. Chem. Soc.*, 1988, **110**, 6913–6914.
56 Z. B. Alfassi, S. Marguet and P. Neta, *J. Phys. Chem.*, 1994, **98**, 8019–8023.
57 Z. B. Alfassi, G. I. Khaikin and P. Neta, *J. Phys. Chem.*, 1995, **99**, 265–268.
58 X. Fang, R. Mertens and C. von Sonntag, *J. Chem. Soc., Perkin Trans. 2*, 1995, 1033–1036.
59 G. I. Khaikin, Z. B. Alfassi and P. Neta, *J. Phys. Chem.*, 1995, **99**, 16722–16726.
60 S. Naumov and C. von Sonntag, *J. Phys. Org. Chem.*, 2005, **18**, 586–594.
61 P. M. Sommeling, P. Mulder, A. Louw, D. V. Avila, J. Lusztyk and K. U. Ingold, *J. Phys. Chem.*, 1993, **97**, 8361–8364.
62 D. V. Avila, J. Lusztyk and K. U. Ingold, *J. Am. Chem. Soc.*, 1992, **114**, 6576–6577.
63 P. Neta, M. Dizdaroglu and M. G. Simic, *Isr. J. Chem.*, 1984, **24**, 25–28.
64 J. Bartl, S. Steenken, H. Mayr and R. A. McClelland, *J. Am. Chem. Soc.*, 1990, **112**, 6918–6928.
65 B. Badger and B. Brocklehurst, *Trans. Faraday Soc.*, 1969, **65**, 2582–2587.
66 A. Kira, S. Arai and M. Imamura, *J. Chem. Phys.*, 1971, **54**, 4890–4895.
67 T. Shida and W. H. Hamill, *J. Chem. Phys.*, 1966, **44**, 4372–4377.